8th Manufacturing Engineering Society International Conference

Analysis of printing parameters for metal additive manufactured parts through Direct Ink Writing process

J. Bonada[a,b,*], E. Xuriguera[c], L. Calvo[a], L. Poudelet[a], R. Cardona[a], J.A. Padilla[c], M. Niubó[c], F. Fenollosa[a]

[a]Centre CIM, Llorens i artigas 12, Barcelona (08028), Spain
[b]Strength of Materials and Structural Engineering Department, Universitat Politècnica de Catalunya, Diagonal 647, Barcelona (08028) Spain
[c]Material Science and Physical Chemistry, Universitat de Barcelona, Martí i Franquès 1, Barcelona (08028), Spain

Abstract

Direct Ink Writing is an Additive Manufacturing process in which a metal ink is continuously extruded to built-up a green metal part. Therefore, a debinding and sintering process is required to obtain the final metal part. This thermal process produces a shrinkage of the green printed part according to several material and printing parameters. In this paper, the influence of printing process planning on the width of printed rods for a copper ink is analyzed by means of a Design of Experiments procedure to optimize the printing and equipment parameters and characterize the shrinkage after the sintering process.

Keywords: Direct Ink Writing; Additive Manufacturing; Printing process planning

1. Introduction

Additive Manufacturing (AM) technologies can produce solid parts adding material layer by layer. Several AM processes could be used to manufacture metal parts, such as Selective Laser Sintering (SLS), Selective Laser Melting (SLM), Direct Ink Writing (DIW), etc. Direct Ink Writing is an AM process in which a viscoelastic ink is continuously extruded through a nozzle. DIW, or also known as Robocasting, could be used for different kind of materials, like

----

* Corresponding author. Tel.: +34-934016226.
E-mail address: jordi.bonada@upc.edu

metals [1,2], ceramics [3,4], biomaterials, etc. When a DIW process is used to manufacture metal or ceramic objects, the printing process produces a green part. Therefore, a drying, debinding and sintering process is required to obtain the final functional object. As a result, the final part could present relevant geometrical changes after the debinding and sintering process as a consequence of the shrinkage of the green part [1]. It is known shrinkage depends on ink rheological properties, solid load content of metal powder, thermic cycle used in the debinding and sintering process [4] and the printing process planning defined during the manufacturing stage [5]. Thus, a properly definition of printing process planning is a key factor to obtain functional parts in terms of geometric tolerances, to avoid non-desired effects (cracks, porous, etc.) as a consequence of the thermal cycle (debinding and sintering) and to make compatible a multimaterial printing process [6].

The use of DIW for metal and ceramic materials has been extended in recent years as a consequence of being a low-cost and accessible technology and its efficiency in the use of raw materials. In fact, the material is dispensed through a syringe; thus the amount of material required depends on the volume of the objective part to be printed. However, DIW presents limitations to print complex structures with large unsupported regions or overhangs. Consequently, the use of supports [6] and origami structures [7] has been investigated in order to solve this issue.

The main goal of this paper is to analyze the influence of printing parameters of a DIW system on the width of printed rods for a copper ink by means of Design of Experiments (DoE) procedure. Afterwards, a slicer algorithm for DIW process is developed and presented to control each printing parameter in order to define a specific printing process planning which will be used to evaluate the shrinkage of the final part after the debinding and sintering process.

2. Direct Ink Writing process for metal inks

The traditional manufacturing workflow necessary to obtain a final part by DIW system is shown in Fig. 1. The AM process begins with the digital file to be printed, traditionally in a STL format. The second step is the manufacturing process of a green part, in which the printing process planning is defined. Most of manufacturing parameters, such as, layer thickness, nozzle diameter, orientation and separation or printed roads (internal structure or infill), use of shells, etc. are introduced during the printing process planning. Open source slicer algorithms are commonly designed for FDM manufacturing process instead of DIW; consequently, its printing process planning definition is not optimized for DIW manufacturing process. The final step is the debinding and sintering process, where a specific thermal cycle is defined according the ink characteristics (material, solid load content, size and shape of particles, etc.). After this third step the final metal part is obtained.
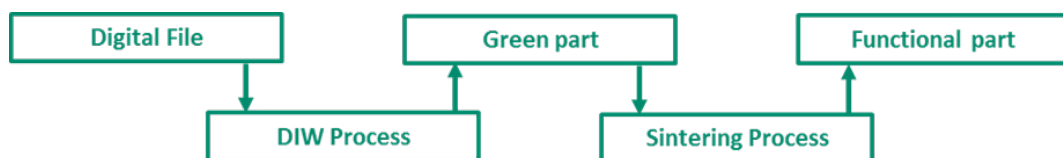

Fig. 1. Main manufacturing steps to obtain a final metallic part through DIW manufacturing process.

2.1. Printing process planning

Printing parameters such as part orientation, layer thickness, internal structure or infill are defined during process planning, and its values have a high influence on the geometry obtained after the printing. Moreover, these printing parameters also have influence on the shrinkage after the sintering process. Thus, a properly definition and optimization of printing process planning would be necessary to predict the effects of sintering, to obtain a full dense part (as much as possible) or a controlled porosity in a lattice structure. Most of printing process planning parameters are commonly introduced in the slicers algorithms to create the machine instructions (Gcode) from the digital file (STL). However, the main open source slicer softwares are focused on Fused Deposition Modelling (FDM) technology. Therefore, it could be difficult to define some specific parameters according to DIW characteristics.

Consequently, a specific slicer procedure for DIW has been developed in order to completely define any printing parameter, infill or any feature necessary during the printing process planning.

The slicer procedure developed have four main steps (Fig. 2). In the first one, the digital file (STL) is converted in a set of black and white images according to the layer thickness; thus, the printable domain of each layer is defined. During the second step, a general structure or infill (stripes, honeycomb, etc.) is also defined also by means of black and white images; consequently, the infill for the objective part could be found through Booleans operations. Furthermore, different internal structures (geometry or separation of rods) for each layer could be used to increase the density of green part and reduce shrinkage after the sintering process. Then, the nozzle trajectories are calculated according to the mechanical features of the DIW equipment. In this third step, all printing process planning parameters could be defined, like manufacturing speed and material flow (or extrusion pressure), globally or for any specific rod, minimizing of movements without material extrusion, inclusion of shells, etc. In the last step, the algorithm transforms all printing parameters and nozzle trajectories to a Gcode file, which could be used in a DIW equipment.
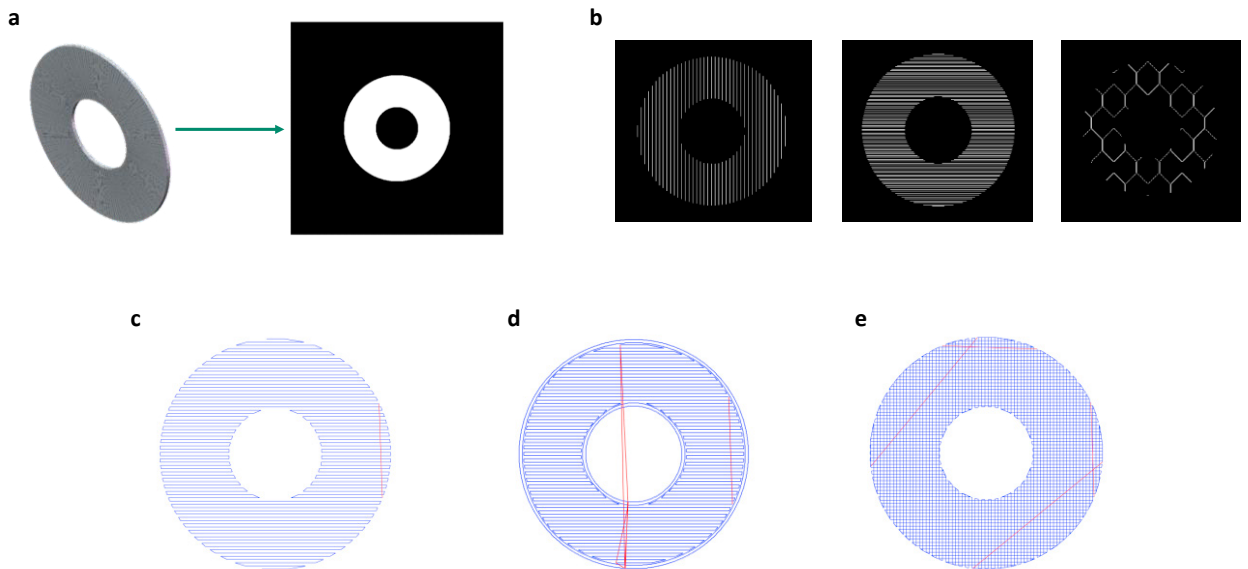

Fig. 2. (a) Set of black and white images from the digital file; (b) Different types of internal structures (vertical stripes, horizontal stripes or honeycomb); (c) nozzle trajectories with the same internal structure for each layer minimizing the movements without material extrusion (red lines); (d) nozzle trajectories for a part with shells; (e) nozzle trajectories for printing process planning with different internal structure in consecutive layers.

2.2.   Copper ink formulation

The copper ink was formulated with a solid content of copper, 35 vol%, added to a Pluronic stock solution. 0.5 wt% of dispersant (Dolapix PC-75), with respect to the solid content, was used. The ink was prepared in a planetary mixer for the dispersion of the particles and elimination of air bubbles in different mixing stages. The ink presents a shear thinning or pseudo plastic behavior that is desirable for Direct Ink Writing inks.

3. Influence of equipment printing parameters on the width of printed rods

In this section the influence of equipment printing settings, mainly manufacturing speed, extrusion pressure and layer thickness on the geometry of a printed rod (width) are analyzed by means of DoE procedure. As a consequence, the printing process planning parameters could be optimized according to the equipment settings in order to obtain a

full dense printed part. As a result, the characterization of the influence of printing process planning on the shrinkage during the sintering process could be properly done.

3.1. Characteristics of DoE

With the purpose of getting the maximum amount of information from the projected tests, an experimental design was made. To develop this study a design of experiments was carried out with Design Expert® software. The DoE technique allows for verifying whether or not there is a synergistic effect between the variables on the final properties of the printed line [8,9]. The main objective of the DoE in this study was to deduce which printing equipment settings have a higher influence on the width of a printed rod. On this manner, it could be obtained the desirable width by adjusting the DIW equipment settings under study, and consequently, the printing process planning parameters (infill) could be properly determined to obtained the desired green part geometry. The three printing settings chosen for analysis were layer thickness (mm), pressure (kPa) and speed (mm/s). The experimental plan performed was a response surface design specifically the Central Composite and it was randomized in order to minimize systematic and accumulative errors on the results. The tests under study are described in Table 1.

The DoE results are based on the analysis of variance (ANOVA) [8]. In this case, p-values have been used to interpret the obtained results. The p-value indicates whether the factor has a significant contribution to the model, represents the smallest level of significance that would lead to rejection of the null-hypothesis (i.e. there is no effect of the controllable factor on the response under investigation) while this hypothesis is true. A p-value lower than the level of significance ($\alpha = 0.05$) indicates significant contribution of the factor with a 95% of confidence. In other words, if a p-value in a test for the significance of a certain factor is smaller than 0.05, this factor is considered statistically significant at $\alpha = 0.05$ level of significance.

Table 1. Experimental plan with equipment settings and results obtained

RUN	Layer Thickness (mm)	Pressure (kPa)	Speed (mm/s)	Width Line (μm)
1	0.4	150	1	1558
1	0.4	150	6	396
2	0.4	150	6	639
4	0.34	180	8	606
5	0.4	200	6	1016
6	0.34	120	8	431
7	0.34	180	3	1083
8	0.46	180	3	1529
9	0.46	120	8	536
10	0.4	150	6	397
11	0.3	150	6	360
12	0.4	150	6	647
13	0.4	150	6	463
14	0.46	180	8	115
15	0.4	150	6	566
16	0.46	120	3	427
17	0.34	120	3	775
18	0.4	150	10	566
19	0.5	150	6	354
20	0.4	110	6	258

3.2. Analysis of DoE results

Table 2 summarizes ANOVA results of the width of printed lines. As it is shown, a significant (p-value<0.0001) statistical quadratic model is obtained. Layer thickness factor does not have a significant effect over the response (p-value=0.8683). Nevertheless, the other variables under study (Pressure and Speed) affect significantly. An increase of extrusion pressure leads to an increase of width line as expected (p-value= 0.0006) and an increase of manufacturing speed leads to a decrease of width line (p-value<0.0001). If both, manufacturing speed and extrusion pressure are increased together, the effect on width line response is found to be higher than the expected of each one separately. In fact, the effect of extrusion pressure enhancing width line is higher at lower speed than at higher manufacturing speed. Hence, it can be concluded that there is a negative interaction between these two variables (p-value=0.0155). These can be also concluded regarding Fig. 3, that shows the width line surface plot obtained. According to the results, an increase of extrusion pressure and manufacturing speed led to an increase of the width of the line being more pronounced with the last mentioned.

Table 2. ANOVA results for width line of the surface response quadratic model.

Source	Sum of squares	df	Mean Square	p-value
Model	2.069E+006	5	4.138E+005	< 0.0001
A-Pressure (kPa)	5.262E+005	1	5.262E+005	0.0006
B-Speed (mm/s)	8.446E+005	1	8.446E+005	< 0.0001
C-Thickness layer (mm)	730.90	1	730.90	0.8683
AB	1.978E+005	1	1.978E+005	0.0155
B2	6.003E+005	1	6.003E+005	0.0003
Residual	3.320E+005	13	25536.91	
Lack of Fit	2.658E+005	8	33230.48	0.1626
Pure Error	66136.00	5	13227.20	
Cor Total	2.401E+006	18		
Model	2.069E+006	5	4.138E+005	< 0.0001

All the results derived from the modification of any of the controllable variables can be translated into a predictive mathematical model. This model can quantitatively foretell a response within the operating range of controllable variables. It can also give some suitable formulations when a certain response is required. The model is shown in Eq. 1.

$$Width = -912.15 + 18.37 \cdot A - 114.06 \cdot B + 123.03 \cdot C - 1.98 \cdot A \cdot B + 28.87 \cdot B^2 \tag{1}$$
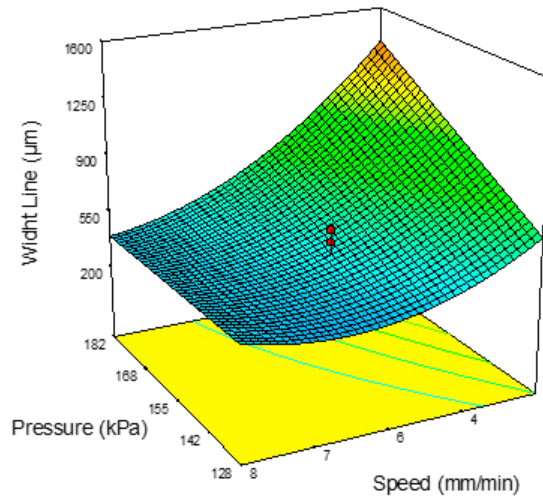
Fig. 3. Response surface plot for width line in function of extrusion pressure and speed for a layer thickness of 0.4 mm.

3.3. Optimization of printing equipment settings

On the basis of the statistical analysis presented above, numerical optimization was performed in order to obtain the optimal results. The basic concept of optimization means a compromise in some values in order to reach higher values in others. The optimization was performed defining a maximal manufacturing speed and allowing some degrees of freedom for the rest of variables.

The goal for the response, based on the mentioned criteria, and two optimum configurations suggested by the model, B1 and B2 are shown in Table 3. In order to evaluate the predictive power of the statistical model composite B1 was tested. Predicted response value is in good agreement with the experimentally obtained value of 497.23 µm.

Table 3. Characteristics of the numerical optimisation.

Name	Goal	Upper Limit	Lower Limit	B1	B2
Speed (mm/s)	Maximize	8.17	2.82	8	8
Pressure (kPa)	In range	179.73	120.27	167	164
Layer thickness (mm)	In range	0.46	0.34	0.37	0.42
Width line (µm)	500	354	1558	499.99	500

4. Analysis of sintering process

Several prismatic pieces of 30x8x4 mm have been printed in order to analyze the shrinkage after the sintering process. The equipment settings defined by model B1 at Section 3.3 have been used to obtain a controlled width rod of 500 µm; therefore, the printing process planning (internal structure) has been properly defined to obtain a full dense, as much as possible, green part. The internal structure defined have one shell, a rod separation of 400 µm (80% of its width, which it is commonly recommended) and different orientation between consecutive layers. Fig. 4 shows the printing process planned obtained though the slicer procedure for the objective part.
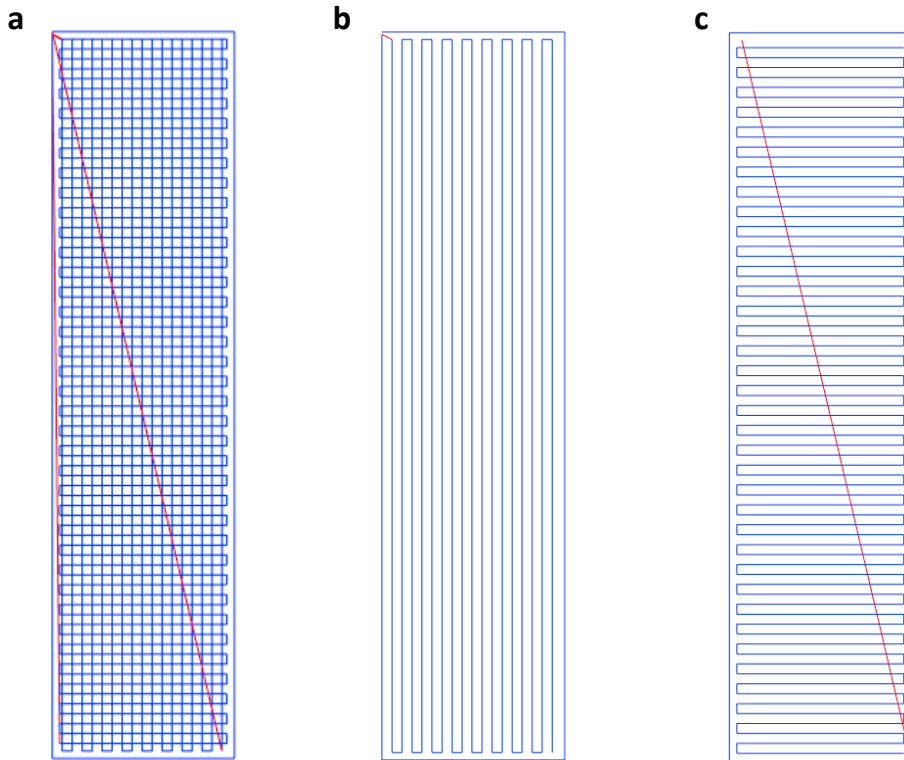
Fig. 4. (a) Nozzle trajectories for all printed layers where the red lines are movements without material extrusion. (b) Internal structure for odd layers. (c) Internal structure for even layers.

In this section the thermal treatment used during the sintering process as well as an initial evaluation of shrinkage for a bulk green part (full dense) are presented. The debinding and sintering process was completed under reducing atmosphere, Ar/5%H$_2$, to avoid the oxidation of the copper pieces. The debinding process was performed at 5ºC/min until 500 ºC with a dwell during 30min, and the sintering process at 5 ºC/min until 950ºC with a dwell of 4 hours. The copper pieces, before and after sintering process can be observed in Fig. 5a and Fig. 5b, respectively. The resulting shrinkage is around 15%. However, a small bending deflection is obtained after the sintering as it can be observed in Fig 5. b.
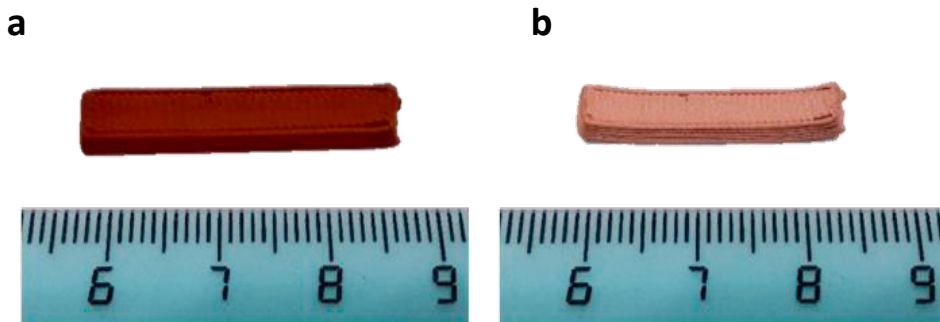

Fig. 5. (a) Green printed part. (b) Final part after the sintering process.

5. Conclusions

A Direct Ink Writing system is used to manufacture copper parts. First of all, a specific slicer procedure to define all printing process planning has been developed in order to properly control the internal structure of metal green parts. Consequently, the internal structure could be optimized to obtain a full dense green part as much as possible. On the other hand, the influence of equipment setting (layer thickness, pressure and manufacturing speed) on the width of printed rod has been evaluated by means of a DoE procedure. The DoE analysis shows a high influence of extrusion pressure and manufacturing speed on the width of a printed rod. Furthermore, a numerical model to predict the width is successfully obtained for a copper ink with a 35% of solid load in volume and the DIW equipment used in this paper. Consequently, the printer settings could be adjusted to obtain a controlled width during the printing process.

A printing process planning, taking into account the results of DoE analysis, has been defined in order to print an objective full dense prismatic piece to evaluate the shrinkage after the sintering process. The results show the viability to obtain a final part using copper ink with a solid load content of 35% in volume. Furthermore, the measured shrinkage after the sintering process is around 15% for the material and printing process planning defined, which it is similar to other manufactured parts through a DIW process using a steel ink with higher solid load content [1,2]. In following steps, the influence of different internal structures and solid load contents on the shrinkage will be evaluated.

Acknowledgements

References

[1] M. Yetna N'Jock, E. Camposilvan, L. Gremillard, E. Maire, D. Fabrègue, D. Chicot, K. Tabalaiev, J. Adrien. Characterization of 100Cr6 lattice structures produced by robocasting. Materials and Design; 121 (2017), 345-354.

[2] C. Xu, Q. Wu, G. L'Espérance, L.L. Lebel, D. Therriault. Enviroment-friendly and reusable ink for 3D printing of metallic structures. Materials and Design; 160 (2018), 262-269.

[3] A. M'Barki, L. Bocquet, A. Stevenson. Linking rheology and printability for dense and strong ceramics by direct ink writing. Scientific Reports 7 (2017), Article number: 6017.

[4] T.Chen, A. Sun, C. Chu, H. Wu, J. Wang, J. Wang, Z. Li, J. Guo. G. Xu. Rheological behavior of titania ink and mechanical properties of titania ceramic structures by 3D direct ink writing using high solid loading titania ceramic ink. Journal of Alloys and Compounds; 783 (2019), 321-328.

[5] U.K. Roopavath, S. Malferrari, A. Van Haver, F. Verstreken, S.N. Rath, D. M. Kalaskar. Optimization of extrusion based ceramic for coplex bony designs. Materials and Design; 162 (2019), 263-270.

[6] C. Xu, B. Quinn, L.L. Lebel, D. Therriault. Multi-material Direct Ink Writing (DIW) for complex metallic structures with removable supports. ACS Appl. Mater, Interfaces; 11 (2019), 8499-8506.

[7] B.Y. Ahn, D. Shoji, C. J. Hansen, E. Hong, D. C. Dunad, J. A. Lewis. Printed origami structures. Advanced Materials; 22 (2010), 2251-2254.

[8] D.C. Montgomery, Design and Analysis of Experiments, 6th Edition Set, John Wiley & Sons, Limited, 2007. https://books.google.es/books?id=x--3PAAACAAJ.

[9] M. Niubó, A.I. Fernández, L. Haurie, X.G. Capdevila, J.M. Chimenos, J.I. Velasco, Influence of the Electric Arc Furnace Dust in the physical and mechanical properties of EVA–polyethylene–butene blends, Mater. Sci. Eng. A. 528 (2011) 4437–4444. doi:10.1016/j.msea.2011.02.006.